Faraday Discussions

Molecular motion in the nanospace of MOFs upon gas adsorption investigated by in situ Raman spectroscopy

Journal:	*Faraday Discussions*
Manuscript ID	FD-ART-01-2020-000002.R1
Article Type:	Paper
Date Submitted by the Author:	27-Jan-2020

Complete List of Authors:	Kusaka, Shinpei; Nagoya University, Department of Chemistry and Biotechnology, School of Engineering Nakajima, Yasuaki; Nagoya University, Department of Chemistry and Biotechnology, School of Engineering Hori, Akihiro; Nagoya University, Department of Chemistry and Biotechnology, School of Engineering Yonezu, Akira; Nagoya University, Department of Chemistry and Biotechnology, School of Engineering Kikushima, Kenta; Nagoya University, Department of Chemistry and Biotechnology, School of Engineering Kosaka, Wataru; Tohoku University, Institute for Materials Research Ma, Yunsheng; Changshu Institute of Technology, Matsuda, Ryotaro; Nagoya University, Department of Chemistry and Biotechnology, School of Engineering

ARTICLE

Molecular motion in the nanospace of MOFs upon gas adsorption investigated by in situ Raman spectroscopy

Received 00th January 20xx,
Accepted 00th January 20xx

DOI: 10.1039/x0xx00000x

Shinpei Kusaka,[a] Yasuaki Nakajima,[a] Akihiro Hori,[a] Akira Yonezu,[a] Kenta Kikushima,[a] Wataru Kosaka,[b] Yunsheng Ma[c] and Ryotaro Matsuda*[ad]

Molecular motions taking place in the nanospace of metal–organic frameworks (MOFs) are an interesting research subject, although not yet fully investigated. In this work, we utilized *in situ* Raman spectroscopy in the ultralow-frequency region to investigate the libration motion (including the rotational motion of phenylene rings) of MOFs, in particular $[Cu_2(bdc)_2(dabco)]$ (Cu-JAST-1), where bdc = 1,4-benzenedicarboxylate and dabco = 1,4-diazabicyclo[2.2.2]octane. The libration mode of Cu-JAST-1 was found to be significantly suppressed by the adsorption of various guest molecules, such as CO_2, Ar, and N_2. In addition, an appreciable correlation between the libration mode and adsorption equilibrium time was identified, which provides useful novel tools in the design of MOFs acting as molecular adsorption and separation materials.

Introduction

Microporous materials, such as metal–organic frameworks (MOFs),[1,2] which are composed of metal ions and organic ligands, have large void spaces in the solid phase, in contrast to most crystalline solids, which have dense packing structures. In such porous materials, the individual ligands are not tightly confined with each other and have high degree of freedom. Indeed, reflecting such structural characteristics, some MOFs have been known to display "flexibility",[3-6] a property whereby the material's skeleton can be transformed, typically as a result of the adsorption and desorption of guest molecules into or from the MOFs' pores. Upon such structural transformation, the cooperative progress of the adsorption of guest molecules and the structural change of the material's skeleton induce a drastic increase in the amount of guest molecules adsorbed, as a consequence of even small pressure changes. Notably, this type of behavior is called gate-opening adsorption.[7] Taking advantage of such characteristic adsorption behavior, flexible MOFs have been extensively studied as potential next-generation adsorbent materials for gas separation.[8-13] The processes involved in guest gas molecule adsorption into MOFs have been observed to be homogeneous within a whole crystal, so they have been studied in detail performing X-ray diffraction measurements and structural analyses under gas atmosphere.[10,13]

Importantly, the high degree of spatial freedom of ligands within the MOF structure also has a significant effect on local molecular motions, such as the vibrations and rotations of ligands in the framework.[14-19] For example, in terephthalic acid-based MOFs like MOF-5, phenylene ring of terephthalate can rotate around the 1,4-positions of terephthalate as a rotation axis.[15-18] Although the molecular motion comprising the described rotation covers a broad range of frequencies, it can be roughly classified into two motions: an independent and local motion, and a harmonic and long-range ordered motion.

A representative example of the former motion is a 180° flip of the phenylene ring, whereas an example of the latter harmonic and long-range ordered motion is a terahertz oscillation of the framework related to the libration mode. The mentioned 180° flip is a relatively slow motion occurring in the 10^3–10^8 Hz frequency range, and it has been studied mainly by solid-state NMR.[15-17] The change of molecular motion may cause the effective pore space, which could affect the adsorption behaviour of MOF. For example, gate-opening adsorption behaviour can be tuned by the state of the rotational motion of the ligand.[19,20] Importantly, this local change in rotational motion does not cause changes in the lattice volume, which is an advantageous feature from the standpoint of the applications of MOFs.

The mentioned terahertz oscillation of the framework is substantially faster than the described 180° flip of the phenylene ring. The libration-related framework oscillation can be monitored by, for instance, Raman spectroscopy[21] or inelastic neutron scattering,[22] focusing on the low-wavenumber region. Over the past few years, as a result of the improvements introduced to the spectroscopic techniques and theoretical calculations, the terahertz motion of porous solids has attracted much research interest.[23,24] However, studies on this motion taking place in MOFs are still limited; in fact, only one report by Stepanov *et al*. exists on the correlation between

[a] *Department of Chemistry and Biotechnology, School of Engineering, Nagoya University, Chikusa-ku, Nagoya 464-8603, Japan.*
[b] *Institute for Materials Research, Tohoku University,2-1-1 Katahira, Aoba-ku, Sendai, 980-8577, Japan,*
[c] *School of Chemistry and Materials Engineering, Jiangsu Key Laboratory of Advanced Functional Materials, Changshu Institute of Technology, Changshu, Jiangsu 215500, PR China.*
[d] *Institute for Advanced Research, Nagoya University, Chikusa-ku, Nagoya 464-8603, Japan. E-mail: ryotaro.matsuda@chembio.nagoya-u.ac.jp*
†Electronic Supplementary Information (ESI) available: General procedures and materials, characterization data, and Raman spectroscopy data. For ESI see DOI: 10.1039/x0xx00000x

MOFs' terahertz motion and adsorption behavior; in the relevant study, ^{2}H NMR spin–lattice relaxation was employed to investigate the libration mode of UiO-66 (Zr) of the guest-free and guest-adsorbed phases.[25] Against this background, as part of the present study, a device enabling users to perform *in situ* Raman spectroscopy measurements in the low-wavenumber region under various gas atmospheres was constructed, and the effect that gas adsorption had on the libration modes of MOFs was studied. Furthermore, we studied the correlation between the adsorption rate of guest molecules and the libration motion of the frameworks.

Experimental section

The general procedures implemented to conduct the experiments described in this report can be found in the ESI.†

Synthesis of MIL-140A

MIL-140A was syhtnesized following reported method. A solution of $ZrCl_4$ (0.25 mmol), terephthalic acid (0.25 mmol) and acetic acid (1.75 mmol) in N,N'-dimethylformamide (2.5 mL) was heated under microwave irradiation at 220 °C for 20 min. Powders were collected by filtration, washed with methanol, and heated at 120 ºC under dynamic vacuum for desolvation.

Synthesis of Cu-JAST-1 [Cu_2(bdc)$_2$(dabco)], Cu-JAST-1D [Cu_2(bdc-d_4)$_2$(dabco)] and Cu-JAST-5 [Cu_2(dmbdc)$_2$(dabco)]

A MeOH (100 mL) solution of dicarboxylic acids (1.0 mmol) {where tereterephthalic acid (H_2bdc) for Cu-JAST-1, terephthalic acid-d_4 (H_2bdc-d_4) for Cu-JAST-1D and 2,3-dimethoxybenzenedicarboxylic acid (H_2dmbdc) for Cu-JAST-5} and formic acid (2 mL) was added a MeOH (100 mL) solution of $Cu(CH_3COO)_2{\cdot}H_2O$ (1.0 mmol), and it was stirred for 2 days at room temperature. The precipitate was filtered off, and added to a solution of MeOH and toluene (1:1, 10 mL) of 1,4-diazabicyclo[2.2.2]octane (dabco) (1.2 mmol), which was heated at 120 ºC at 24 h in a teflon-lined stainless-steel autoclave bomb. Powders were collected by filtration and heated at 120 ºC under dynamic vacuum for desolvation.

Adsorption: instruments and measurements

Measurements to obtain adsorption isobars, isotherms, and rates were performed using a microtrac-BEL BELSORP-18 automated volumetric gas adsorption analyser equipped with a cryostat from ULVAC-cryo. Before measurements were performed, each sample was dried under dynamic vacuum at 393 K for 5 h. The isobars were measured between 298.15 K and the boiling temperature of each gas with a 5 K steps. Adsorption rate analysis was performed adopting the linear driving force (LDF) approximation by fitting the time-course change of the pressures during adsorption processes. The mass transfer coefficient $k_s a_p$ (s^{-1}) was obtained *via* the following equation:

$$\frac{p-p_{\mathrm{en}}}{p_0-p_{\mathrm{en}}} = 1-\left(\frac{p_0-p_{\mathrm{en-1}}}{p_0+p_{\mathrm{en}}}\right)\left(\frac{\alpha}{\alpha+1}\right)\left[1-\exp\left\{-\left(\frac{\alpha+1}{\alpha}\right)k_s a_p t\right\}\right],$$

where p is the pressure, p_{en} is the equilibrium pressure, $p_{\mathrm{en-1}}$ is the equilibrium pressure of the previous data point, p_0 is the starting pressure, α is the distribution coefficient, and t is the time.

Raman measurements in the ultralow-wavenumber region

A device allowing to perform Raman spectroscopy measurements *in situ* at variable temperatures and gas atmosphere was constructed by connecting a cryostat (4 K GM refrigerator) to a HORIBA LabRAM HR Evolution microscopic Raman spectrometer with a focal length of 800 mm. Quartz windows were equipped over the sample room and the vacuum insulation shield of the cryostat. Through the window, samples were inspected using a microscope (Olympus SLMPLN20x) and irradiated with a 532 nm Raman excitation laser. The LabRAM HR microscopic Raman spectrometer was equipped with a Si-based, Peltier-cooled charge-coupled device detector, an ultralow-frequency module triple notch filter and a grating (1800 gr/mm) to afford the observation of the low-wavenumber region.

Theoretical calculations

Theoretical calculations were performed using the Gaussian09W software. The model structure was optimized performing B3LYP/6-31G-level calculations, before the frequency calculation was performed. The obtained vibrational frequency was corrected using a scale factor of 0.962.[26]

Results and discussion

Adsorption properties of MIL-140A and Cu-JAST

MIL-140A,[27] Cu-JAST-1[28] and its derivatives were synthesized *via* the reported methods and characterized by powder X-ray diffraction (Fig. S1 and S2) and thermogravimetric analysis (Fig. S3). MIL-140A consists of a three-dimensional framework constructed from a one-dimensional structure of zirconium oxide rods crosslinked with terephthalate. Cu-JAST-1 has a pillared-layer structure in which two-dimensional sheets composed of copper(II) paddle-wheel units and terephthalate are pillared by diazabicyclo[2.2.2]octane (dabco). The N_2 adsorption isotherms of both compounds have been reported, and both frameworks have been shown to display microporosity.

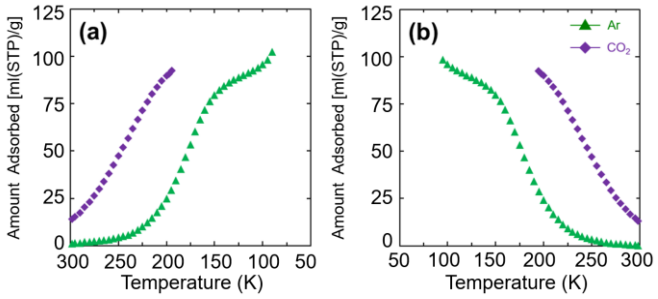

Fig. 1. Adsorption isobars of MIL-140A at 1 bar for (a) cooling and (b)heating processes.

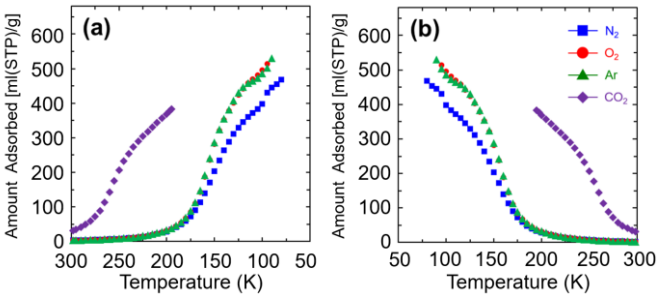

Fig. 2. Adsorption isobars of Cu-JAST-1 at 1 bar for (a) cooling and (b) heating processes.

Notably, the temperature dependence of guest molecule adsorption by these compounds under conditions of constant pressure has not been studied. The adsorption isobars of MIL-140A and Cu-JAST-1 at 1 bar gas pressure were obtained using various gases (Fig. 1 and Fig. 2, respectively). Pre-dried MIL-140A was found to adsorb CO_2 at 300 K, and the amount of adsorbed gas was found to increase as the temperature decreased. The maximum uptake of CO_2 by MIL-140A was 93 cm^3/g, at a temperature near the boiling point of the gas. The amount of Ar adsorbed by MIL-140A also rapidly increased between 200 and was saturated at ~90 K (103 cm^3/g). Conversely, as the temperature increased, both CO_2 and Ar were desorbed from MIL-140A in the absence of hysteresis. MIL-140A exhibited adsorption at very low relative pressure, and no hysteresis was observed during the adsorption and desorption processes, indicating that MIL-140A is characterized by rigid micropores.

In the case of Cu-JAST-1, adsorption isobars were measured for N_2, O_2, Ar, and CO_2. Similarly to MIL-140A, a sharp increase in the amount of adsorbed gas was observed as the temperature decreased. Furthermore, no hysteresis was observed during the adsorption and desorption processes, indicating that Cu-JAST-1 is also a microporous material with a rigid framework. The maximum adsorption values were 468, 514, 531, and 384 cm^3/g for N_2, O_2, Ar, and CO_2, respectively. The adsorption capacity of Cu-JAST-1 was higher than that of MIL-140A, and the sudden guest uptake started at lower temperatures, which supports that Cu-JAST-1 has larger pores than MIL-140A.

Raman spectrometry measurements of N_2, O_2, and CO_2

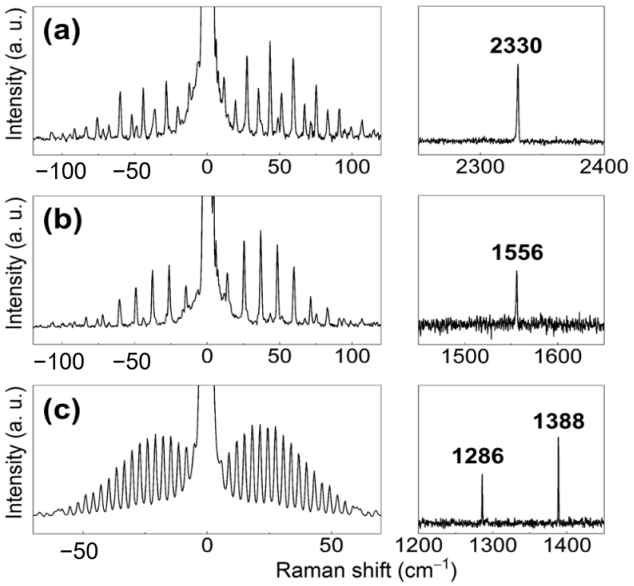

Fig. 3. Raman spectra of (a) N_2, (b) O_2, and (c) CO_2 for pure rotational (left) and vibrational (right) modes.

We initially collected the Raman spectra of N_2, O_2, and CO_2 in the gas phase. As shown in Fig. 3, the pure rotational Raman spectra of each molecule in the gas phase were clearly observed in the extremely low-wavenumber region (<100 cm^{-1}). The peaks corresponding to the symmetric stretching and the pure rotational modes of the molecules are in good agreement with those reported, and the rotation constants obtained from the line spacing of each pure rotational Raman spectrum are also consistent with the values reported in the literature (Table S1), which is indicative of the high accuracy of the device in the extremely low-wavenumber region.

Raman spectrometry measurements on MIL-140A

The experimental and simulated Raman spectra of MIL-140A were reported by Tan *et al*.[23] However, the experimental Raman spectrum was very broad, and some peaks in the ultralow-wavenumber region did not match well those of the simulated one. Therefore, we recorded the Raman spectrum of MIL-140A at room temperature using our device and examined the feasibility of monitoring of the libration mode of MOFs. The experimental spectrum thus obtained was in very good agreement with the calculation results (Fig. S4). In particular, two peaks at 44.69 cm^{-1} (1.34 THz) and 49.22 cm^{-1} (1.48 THz) assigned to one of the two rotor libration modes (asymmetric and symmetric type-A rotor)[23] are clearly separated, which is indicative of the high resolution of the spectrum. The peak corresponding to the other rotor libration mode (type B[23]), which appears at ~90 cm^{-1}, overlaps with other peaks. Thus, the libration of type-A rotor was used in the subsequent discussion.

Raman spectroscopy measurements on Cu-JAST-1, Cu-JAST1D and Cu-JAST-5

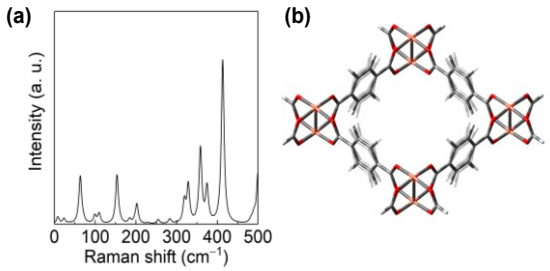

Fig. 4. (a) The simulated Raman spectrum of a model structure of Cu-JAST-1. (b) Illustration of the libration mode of the model structure of Cu-JAST-1 at 61.12 cm^{-1} frequency.

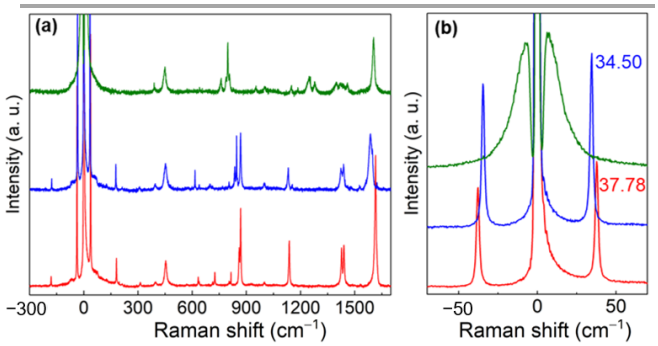

Fig. 5. (a) Full-range and (b) Low wavenumber region zoom-up Raman spectra of Cu-JAST derivatives at room temperature in an air atmosphere (red: Cu-JAST-1, blue: Cu-JAST-1D, green: Cu-JAST-5).

In order to estimate the features of the Raman spectrum of Cu-JAST-1, theoretical calculations were performed by a density functional theory-based approach using a discrete model structure whereby four Cu paddle-wheel units are interconnected by four terephthalate end-capped with formate units (Fig. 4). Based on this assumption, a libration mode of the phenylene rings of terephthalates was estimated to give rise to a Raman peak in the low-frequency region (61.12 cm^{-1}).

Subsequently, Raman spectroscopy measurements were performed on Cu-JAST-1, Cu-JAST-1D, and Cu-JAST-5 under an air atmosphere at room temperature (Fig. 5). The peaks at ~450 cm^{-1}, which were observed for each compound, were assigned to the vibration mode of Cu and terephthalate around the paddle-wheel unit. In addition, for all three compounds, a very intense peak was observed in the low-wavenumber region of the spectrum, which can be assumed to correspond to the peak of the libration mode. The peak appeared at lower frequency (3.28 cm^{-1}) for Cu-JAST-1D than for Cu-JAST-1. This observation can be explained as descending from the fact that the deuterated phenylene ring has a larger inertia moment than its non-deuterated counterpart. The Raman peak of the libration mode of Cu-JAST-5 shifted to even lower frequency, and it was quite broad. The asymmetry of the 1,2-dimethoxyphenylene moiety is such that multiple spatially stable conformations with different energy levels are possible.

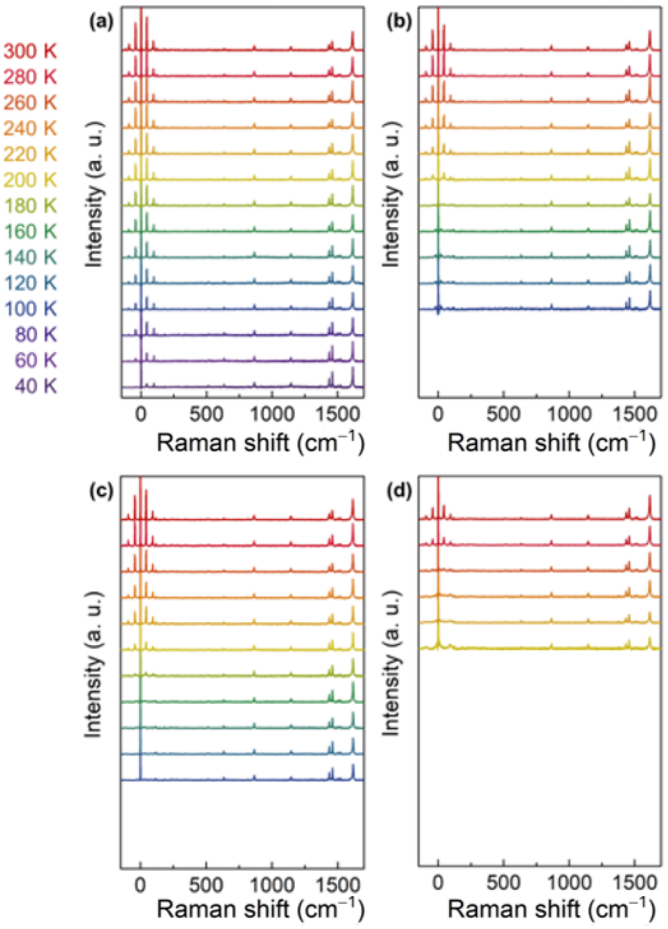

Fig. 6. Temperature dependent Raman spectra of MIL-140 A under (a) He (b) Ar (c) N_2 (d) CO_2 at 100 KPa. The peak intensity was normalized using the peak at 800 cm^{-1} as the standard.

Therefore, we assumed that the peaks due to libration modes with different energy levels overlapped to form a broad peak.

***In situ* Raman spectroscopy measurements under gas atmosphere**

In order to investigate the effect that gas adsorption has on the libration modes of MIL-140A and Cu-JAST-1, *in situ* Raman spectra measurements were performed on these frameworks under He, Ar, N_2, O_2, and CO_2 gas atmosphere at 100 kPa as the temperature was decreased (Fig. 6 and 7, respectively).

In the cases of both MIL-140A and Cu-JAST-1, the peaks in the high-wavenumber region (>300 cm^{-1}) did not change, indicating that the frameworks maintained their structural features during the gas adsorption process. On the other hand, the peak due to the libration mode that appears in the low-wavenumber region changed significantly depending on the gas and the temperature (Fig. S5 and S6). For both MIL-140A and Cu-JAST-1, the peak gradually diminished in intensity as the temperature decreased. The peak finally disappeared at 160 K when the gases were Ar, N_2, and O_2, and it did so at 240 K when the gas was CO_2, a temperature value much higher than that observed for He (<40 K) (Fig. S7 and Fig. S8).

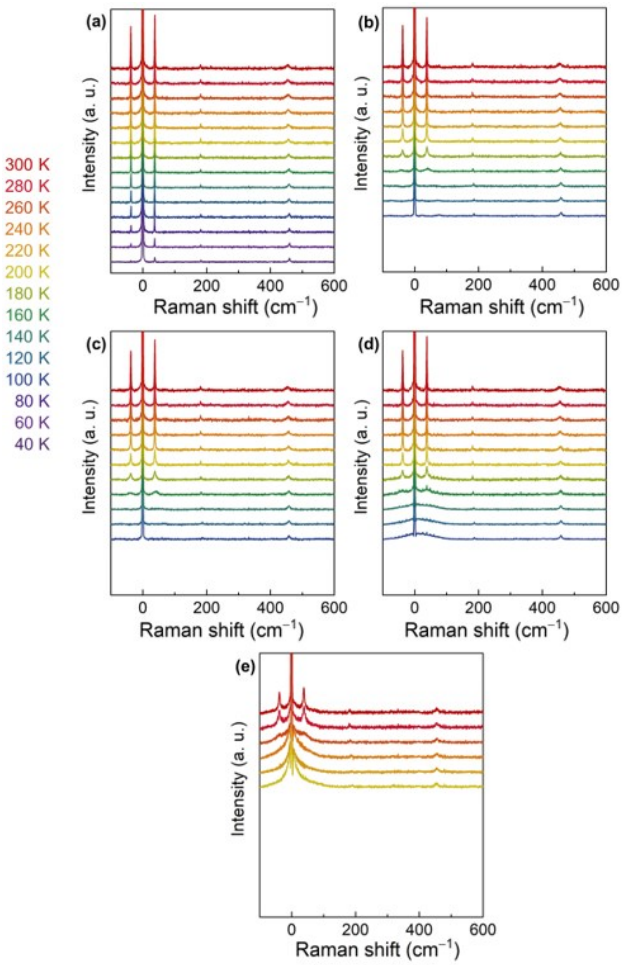

Fig. 7. Temperature dependent Raman spectra of Cu-JAST-1 under (a) He (b) Ar (c) N_2 (d) O_2 (e) CO_2 atmosphere (100 KPa). The peak intensity was normalized using the peak at 450 cm^{-1} as the standard.

Comparing these data with the adsorption isobars (Fig. 1 and 2), the temperatures at which the peaks due to the libration mode disappeared correspond to the temperatures at which the values for guest molecule adsorption were in the 50–75 cm^3/g range for MIL-140A and in the 150–250 cm^3/g range for Cu-JAST-1, regardless of the specific gas. Since the phenylene ring may not have a specific interaction with the used gases, it is suggested that the motions involved in the libration mode are sterically hindered when the density of gas molecules adsorbed in the pores of the framework is above a certain threshold.

In addition to the mentioned decrease in intensity, as the temperature decreased, a broadening of the peak associated with the libration mode was also observed. In contrast to the peak intensity, which decreased linearly with the temperature, the full width at half maxima (FWHM) of the peaks displayed a sudden increase in value at specific temperatures, suggesting the existence of a strong correlation between the FWHM value and the amount of gas adsorbed (Fig. 8 and 9).

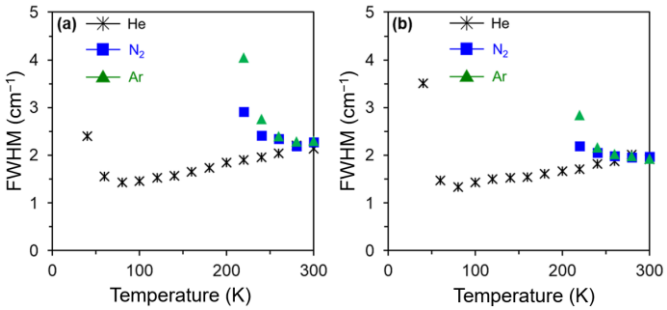

Fig. 8. Temperature dependence of the value of the full width at half maxima (FWHM) of the Raman peak of the libration mode for MIL-140A in He (black), N_2 (blue) and Ar (green).

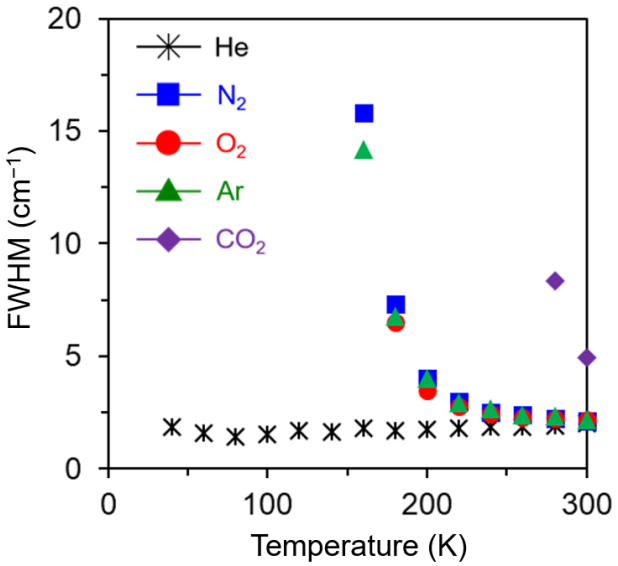

Fig. 9. Temperature dependence of the value of the full width at half maxima (FWHM) of the Raman peak of the libration mode in Cu-JAST-1 in He (black), N_2 (blue) O_2 (red), Ar (green) and CO_2 (purple).

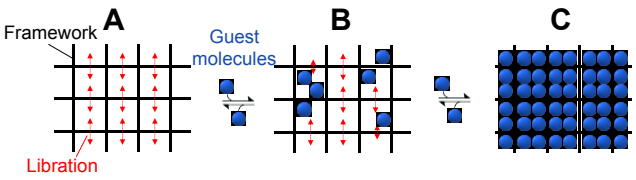

Fig. 10. Schematic illustration of the changes the libration mode undergoes following guest molecule adsorption in a MOF.

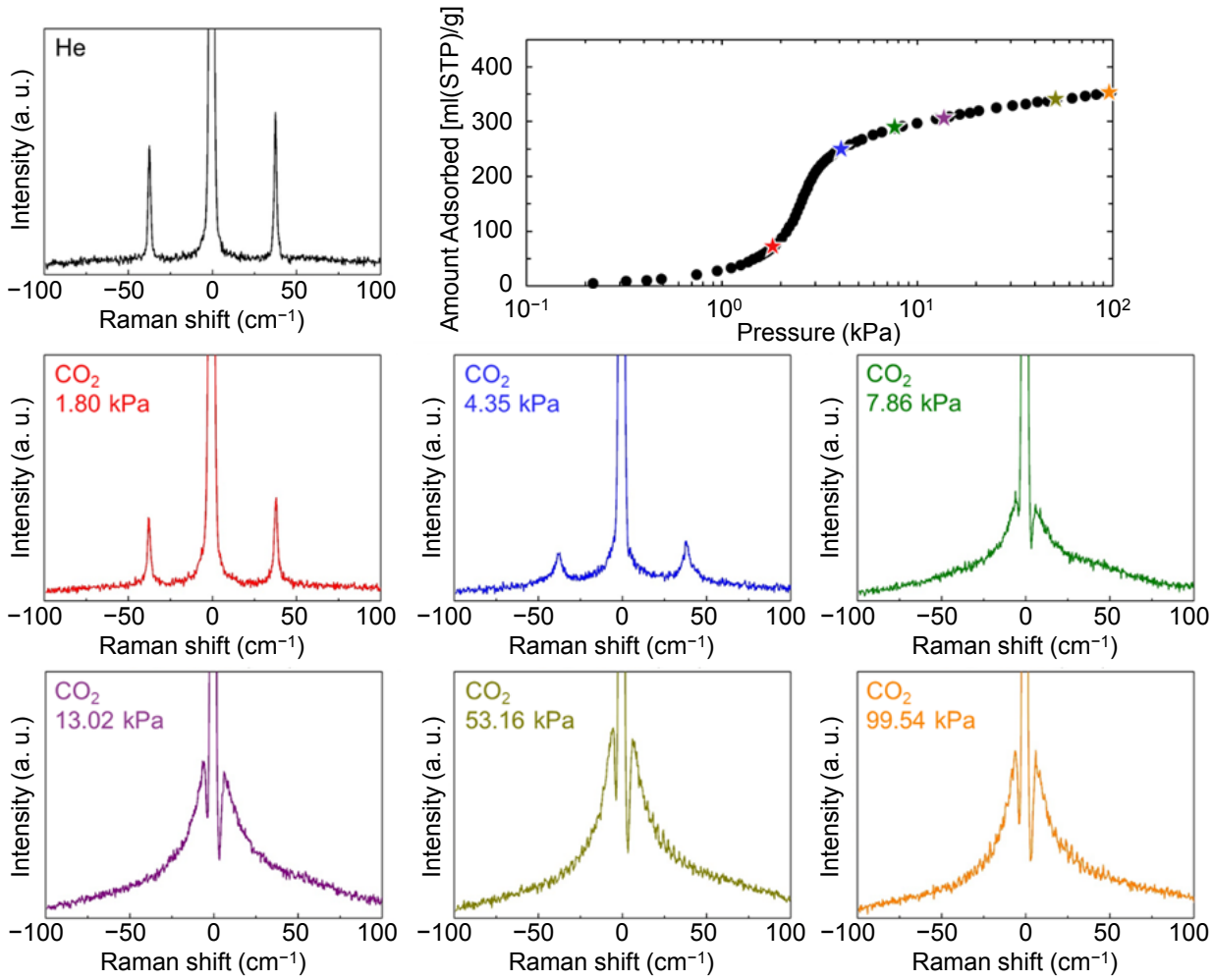

Fig. 11. Pressure dependent Raman spectra of Cu-JAST-1 under CO_2 at 194.7 K. Upright shows the adsorption isotherm of Cu-JAST-1 and the colored stars are data points where Raman spectra were measured.

In general, the FWHM value of a Raman spectrum peak is correlated with the uniformity of the corresponding mode. When gas molecules are not adsorbed in the pores, the libration mode of MOFs can take place over a large domain of the crystal as a uniform harmonic mode (scenario A in Fig. 10). When gas molecules start to be adsorbed into the MOF, the motion of the phenylene ring is partially hindered, so that the libration mode becomes heterogeneous over multiple domains (scenario B in Fig. 10), and the FWHM value of the relevant Raman peak increases. Ultimately, when the pores are completely filled with gas molecules (scenario C in Fig. 10), the motion of the libration mode is lost, and the relevant Raman peak disappears. Evidence thus indicates that molecule adsorption in the pores strongly affected the libration mode.

The state of adsorbed guest molecules

In the experiment of Cu-JAST-1 in CO_2 atmosphere, in addition to the sharp peak assigned to the libration mode, another broad peak appeared around Rayleigh light. This peak is different from those of the phonon mode of solid and pure rotation of gaseous CO_2 (Fig. S9), but it is rather similar to that of the liquid phase, which cannot normally exist under the described conditions.

The dependence of the Raman spectra on CO_2 pressure at 194.7 K was also investigated (Fig. 11). As observed in the case of the temperature-dependent Raman spectra recorded at constant pressure, the peak associated with the libration mode disappeared as the pressure value increased (leading also to an increase in the amount of CO_2 adsorbed into the Cu-JAST-1). At the same time, the broad peak discussed above similarly appeared around the Rayleigh light (Fig. S10). The Raman spectra of Cu-JAST-1 under varying O_2 pressure showed similar behavior to those recorded under varying CO_2 pressure; by contrast, when the corresponding experiments were conducted under Ar and N_2, new sharp peaks were observed to appear as the gas pressure increased (Fig. S10), which were likely to be assignable to solid phonon modes.

Kinetics and adsorptions

As discussed above, the libration mode of the framework diminished and ultimately disappeared as a result of the adsorption of gas molecules into the MOFs. Conversely, we hypothesized that the molecular adsorption behavior may be correlated with changes in the libration mode. Therefore, we calculated the mass transfer coefficient ($k_s a_p$), which correlates to the diffusion rate of gas

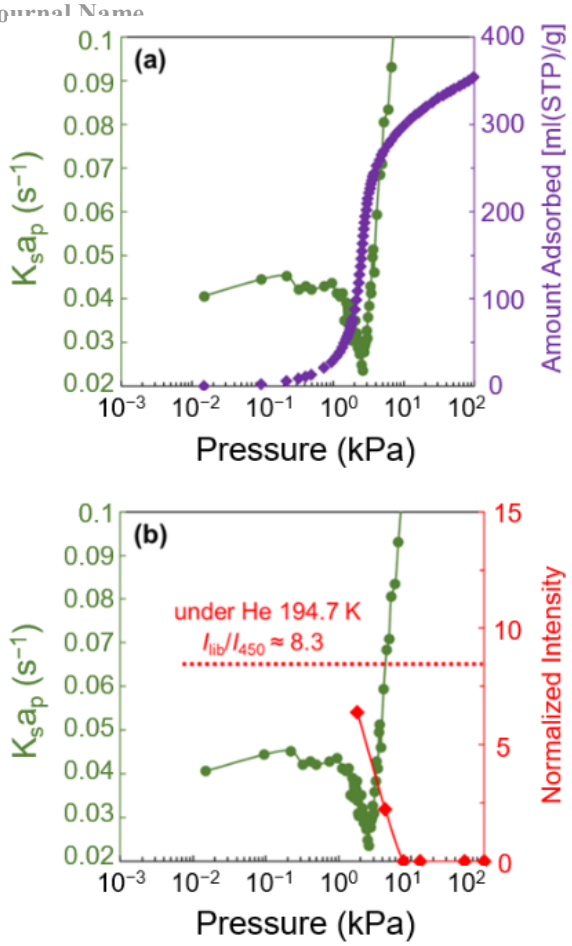

Fig. 12. Overlay plots for the $k_s a_p$ values (green) and (a) the adsorption isotherm of CO_2 for Cu-JAST-1 (purple) or (b) the Raman peak intensity of the libration mode (I_{lib}) normalized with that at 450 cm^{-1} (I_{450}) (red). The red dotted line corresponds I_{lib}/I_{450} for guest-free Cu-JAST-1 at 194.7 K, which has been observed under He at 1 bar.

molecules in the pore, at each data point in the adsorption isotherm of CO_2 for Cu-JAST-1 at 195 K. The value of $k_s a_p$ was found to begin decreasing sharply at ~1.0 Pa, reaching a minimum at ~3.0 Pa. As pressure rose further, the value of $k_s a_p$ started to increase (Fig. 12). Comparing this change in the value of $k_s a_p$ with the adsorption isotherm, one can evince that the drop in $k_s a_p$ value occurs in the pressure region where the amount of gas molecules adsorbed starts to increase sharply, and it becomes smallest when adsorption reaches a level that is about half that of saturation. In addition, comparing the intensity of the libration mode with the value of $k_s a_p$, one can infer that the decrease in $k_s a_p$ value also occurred when the intensity of the libration mode decreased. In other words, molecular diffusion slows down early during the adsorption process (ongoing from the scenario A to the scenario B in Fig. 10), and it subsequently speeds up after the pore is filled to some extent (ongoing from the scenario B to the scenario C in Fig. 10). We thus suggest that the diffusion of gas molecules in the pore is hindered by the non-uniformity of the libration mode.

Conclusions

The correlation between the motion of the MOFs and guest molecule adsorption is an interesting research subject. In particular, the MOFs' molecular motions in the terahertz region fall in an area of the Raman spectrum that has not been investigated so far.

In this work, we performed *in situ* high resolution Raman spectroscopy measurements of MOFs kept under various pure gases to probe the libration mode involving the rotation of the MOFs' phenylene rings, and we found this mode to be frozen once the temperature of the system descended to 40 K or the adsorbed gas exceeded half of the adsorption capacity. We also observed a broadening of the relevant peaks in the Raman spectra, which suggests that the libration mode becomes non-uniform as guest gas molecules are adsorbed into the pores of the MOFs. Furthermore, we found that the guest gas molecule diffusion rate in the MOFs and the intensity of the libration mode were decreased in accordance with the gas adsorption in the pores, suggesting that a non-uniform libration mode inhibits molecular diffusion. We believe that the identification of such a correlation between the libration mode and adsorption equilibrium time will enable researchers to draft new guidelines for the design of MOFs having molecular separation abilities related to molecular diffusion.

Conflicts of interest

There are no conflicts to declare.

Acknowledgements

This work was supported by the PRESTO (Grant No. JPMJPR141C) and CREST (Grant No. JPMJCR17I3) of the Japan Science and Technology Agency (JST), and JSPS KAKENHI Grant Numbers JP16H06032, JP17H03122, JP18K14043, JP18K05145, and JP19H02734.

Notes and references

1 S. Kitagawa, *Acc. Chem. Res.*, 2017, **50**, 514–516.
2 C. S. Diercks, M. J. Kalmutzki, N. J. Diercks and O. M. Yaghi, *ACS Cent. Sci.*, 2018, **4**, 1457.
3 Y. Zhang, X. Zhang, J. Lyu, K. I. Otake, X. Wang, L. R. Redfern, C. D. Malliakas, Z. Li, T. Islamoglu, B. Wang and O. K. Farha, *J. Am. Chem. Soc.*, 2018, **140**, 11179.
4 S. Wannapaiboon, A. Schneemann, I. Hante, M. Tu, K. Epp, A. L. Semrau, C. Sternemann, M. Paulus, S. J. Baxter, G. Kieslich and R. A. Fischer, *Nat. Commun.*, 2019, **10**, 346.
5 A. P. Katsoulidis, D. Antypov, G. F. S. Whitehead, E. J. Carrington, D. J. Adams, N. G. Berry, G. R. Darling, M. S. Dyer and M. J. Rosseinsky, *Nature*, 2019, **565**, 213.
6 S. Krause, V. Bon, I. Senkovska, U. Stoeck, D. Wallacher, D. M. Tobbens, S. Zander, R. S. Pillai, G. Maurin, F. X. Coudert and S. Kaskel, *Nature*, 2016, **532**, 348.
7 A. Kondo, H. Noguchi, L. Carlucci, D. M. Proserpio, G. Ciani, H. Kajiro, T. Ohba, H. Kanoh and K. Kaneko, *J. Am. Chem. Soc.*, 2007, **129**, 12362.
8 S. Mukherjee, B. Joarder, B. Manna, A. V. Desai, A. K. Chaudhari and S. K. Ghosh, *Sci. Rep.*, 2014, **4**, 5741.
9 C. Gücüyener, J. van den Bergh, J. Gascon and F. Kapteijin, *J. Am. Chem. Soc.*, 2010, **132**, 17704.

10 H. Sato, W. Kosaka, R. Matsuda, A. Hori, Y. Hijikata, R. V. Belosludov, S. Sakaki, M. Takata and S. Kitagawa, *Science*, 2014, **343**, 167.
11 L. Zhang, K. Jiang, L. Li, Y. –P. Xia, T. –L. Hu, Y. Yang, Y. Cui, B. Li, B. Chen and G. Qian, *Chem. Commun*., 2018, **54**, 4846.
12 S. Bhattacharyya, A. Chakraborty, A. Hazra and T. K. Maji, *ACS Omega*, 2018, **3**, 2018.
13 D. A. Reed, B. K. Keitz, J. Oktawiec, J. A. Mason, T. Runčevski, D. J. Xiao, L. E. Darago, V. Crocellà, S. Bordiga and J. R. Long, *Nature*, 2017, **550**, 96.
14 S.Horike, R. Matsuda, D. Tanaka, S. Matsubara, M. Mizuno, K. Endo and S. Kitagawa, *Angew. Chem. Int. Ed*., 2006, **45**, 7226.
15 C. S. Vogelsberg, F. J. Uribe-Romo, A. S. Lipton, S. Yang, K. N. Houk, S. Brown and M. A. Garcia-Garibay, *Proc. Natl. Acad. Sci*., 2017, **52**, 13613.
16 S. Bracco, F. Castiglioni, A. Comotti, S. Galli, M. Negroni, A. Maspero and P. Sozzani, *Chem. –Eur. J.* 2017, **23**, 11210.
17 S. Devautour-Vinot, G. Maurin, C. Serre, P. Horcajada, D. P da Cunha, V. Guillerm, E. D. Costa, F. Taulelle and C Martineau, *Chem. Mater*., 2012, **24**, 2168.
18 J. T. Damron, J. Ma, R. Kurz, K. Saalwächter, A. J. Matzger and Ramamoorthy, *Angew. Chem. Int. Ed*., 2018, **57**, 8678.
19 K. Bärwinkel, M. M. Herling, M. Rieß, H. Sato, L.Li, Y. S. Avadhut, T. W. Kemnitzer, H. Kalo, J. Senker, R. Matsuda, S. Kitagawa and J. Breu, *J. Am. Chem. Soc*., 2017, **139**, 904.
20 M. Inukai, M. Tamura, S. Horike, M. Higuchi, S. Kitagawa and K. nakamura,. *Angew. Chem. Int. Ed*., 2018, **57**, 8687.
21 A. Krylov, A. Vtyurin, P. Petkov, I. Senkovska, M. Maliuta, V. Bon, T. Heine, S. Kaskel and E. Slyusareva, *Phys. Chem. Chem. Phys*., 2017, **19**, 32099.
22 M. R. Ryder, B. Civalleri, T. D. Bennett, S. Henke, S. Rudić, G. Cinque, F. Fernandez-Alonso and J. –C. Tan, *Phys. Rev. Lett*. 2014, **113**, 215502.
23 (a) M. R. Ryder, B. V. de Voorde, B. Civalleri, T. D. Bennett, S. Mukhopadhyay, G. Cinque, F. Fernandez-Alonso, D. De Vos, S. Rudić and J. –C. Tan, *Phys. Rev. Lett*., 2017, **118**, 255502. (b) The details of the motion of Type A and B were shown in the supplement information of this reference 23.
24 A. E. J. Hoffman, L. Vanduyfhuys, I. Nevjestić, J. Wieme, S. M. J. Rogge, H. Depauw, P. Van Der Voort, H. Vrielinck, V. Van Speybroeck and V. V. Speybroeck, *J. Phys. Chem. C*, 2018, **122**, 2734.
25 A. E. Khudozhitkov, H. Jobic, D. I. Kolokolov, D. Freude, J. Haase and A. G. Stepanov, *J. Phys. Chem. C*, 2017, **121**, 11593.
26 https://cccbdb.nist.gov/vibscalejust.asp
27 V. Guillerm, F. Ragon, M. Dan-Hardi, T. Devic, M. Vishnuvarthan, B. Campo, A. Vimont, G. Clet, Q. Yang, G. Maurin, G. Férey, A. Vittadini, S. Gross and C. Serre, *Angew. Chem. Int. Ed*., 2012, **51**, 9267.
28 K. Seki, S. Takamizawa and W. Mori, *Chem. Lett*., 2001, **30**, 332.

TOC Figure